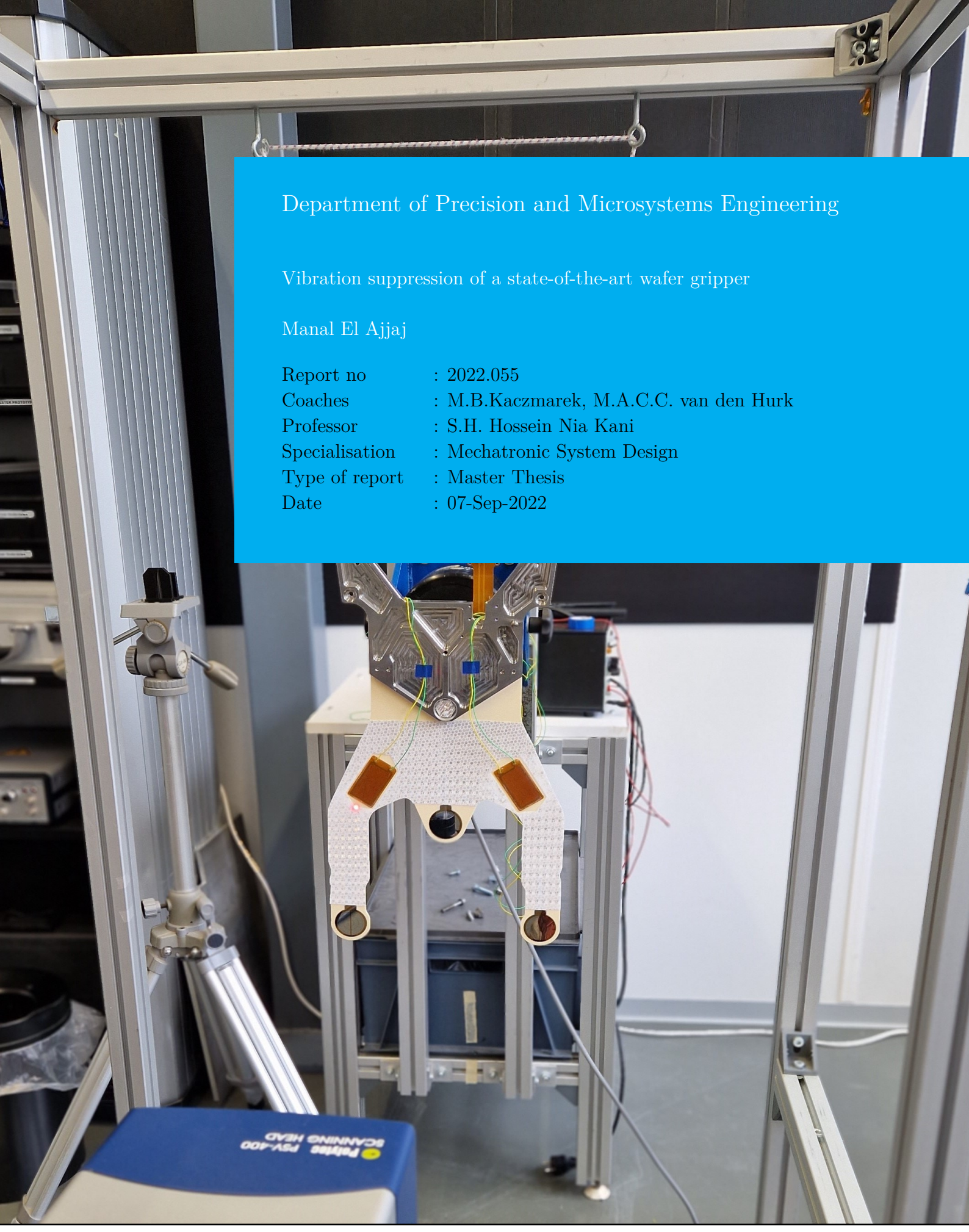

Department of Precision and Microsystems Engineering

Vibration suppression of a state-of-the-art wafer gripper

Manal El Ajjaj

Report no	: 2022.055
Coaches	: M.B.Kaczmarek, M.A.C.C. van den Hurk
Professor	: S.H. Hossein Nia Kani
Specialisation	: Mechatronic System Design
Type of report	: Master Thesis
Date	: 07-Sep-2022

Abstract

Vibration suppression of flexible end-effectors has become one of the great challenges within the semiconductor industry to achieve the precision required to produce chips. These end-effectors tend to be prone to vibrations due to their lightweight design and low thickness, whilst they still should have high accuracy and precision. This motivates the search for damping methods that can be implemented in industry, where the emphasis is set at the upcoming trend in the use of smart materials and structures. In this thesis, the application of piezoelectric transducers to a wafer gripper with a high stiffness is investigated. The main aim is to show a 'proof-of-concept'. This to show the feasibility of piezoelectric transducers that are used to effectively dampen modes of thin and stiff end-effectors. The dynamics of the gripper have been analyzed to determine to optimal placement of the piezoelectric transducers using the coupling relation between the gripper and the transducers. This relation has been studied to be used as a guideline for the design process. After the placement of the piezoelectrics, an experimental setup has been built to perform active vibration control. 3.3% damping was achieved with a simple PPF controller with a limited gain for which the piezoelectric transducers where placed according to a simplified line optimization. This shows that the concept of dampening very stiff and thin end-effectors, such as the wafer gripper, is feasible.

Contents

1 Introduction

The demand for thin lightweight structures has been ever increasing, which leads to new challenges on vibration control technology. This especially holds for the semiconductor industry where high standards are set when it comes to speed, precision and alignment accuracy. The incentive for this growing demand and competitiveness is Moore's Law, which states that every two years the number of transistors per integrated circuit doubles [1]. However, scaling the transistors has become less straightforward and more challenging over the years, whilst companies aim for fast and precise manufacturing. With this, the need for new developments in the field of vibration suppression arises.

One of the main challenges are on flexible robot end-effectors, such as wafer grippers, that tend to be prone to vibrations due to their lightweight design and low thickness. Additionally, the contact between the wafer and the gripper tends to be friction-based. When vibrations are not attenuated for these thin end-effectors, the wafer can slip which destroys the alignment accuracy. In the worst case the wafer breaks or gets lost in the lithography machine. In many flexible structures, only a few vibration modes are significant, so vibration can be controlled by controlling only a certain number of modes. Current solutions have been to increase the thickness of the grippers as much as possible within budget, add mass-spring dampers or to add viscoelastic material to the gripper, see Sections 1.1.1 and 1.1.2. However, these solutions only work up until a certain point and tend to provide limited damping. Smart materials, which are characterized by their coupling between different physical domains, are currently being researched to provide new methods to contribute to vibration attenuation [2]. These smart materials can be integrated in a so called 'smart structure', that can reduce structural vibrations through the high degree of integration of sensors, actuators and an appropriate control system [3].

Therefore, the objective is to propose and validate a solution method, which includes a mechanical design and control system, to achieve at least 5% damping for two eigenmodes of a wafer gripper. The aim here is to dampen two modes of the wafer gripper for a frequency range up to 100Hz by implementing active vibration control with the use of a smart material. This objective serves as a 'proof of concept' to show the possibilities of implementing a state-of-the-art damping method to an industrial application, which in turn can be used to dampen different thin structures. This to see how smart materials and structures can be used to dampen the wafer gripper. It should be noted that there are few applications of the implementation of smart materials, especially to an industrial application. In this report a case for the company VDL ETG will be considered, where vibrations of a wafer gripper need to be suppressed to prevent the excitation of its first two eigenmodes. The case is based on their wafer handler module. This module consists of a typical SCARA robot that handles wafers in vacuum, transporting them to and from the main lithography stage.

1.1. Problem context

The dynamic amplitude of the eigenmodes can cause wafer slip to happen and also disrupts the alignment accuracy of the wafer. Vibrations are being transmitted to the vacuum wafer handler coming from the base module which is depicted in Figure 1.1. Measures to prevent the vibrations of the base module from reaching the wafer handler have already been taken, through decoupling the two systems. However, even after the decoupling, motion is still transferred to the wafer handler. These vibrations

are such that the low frequency eigenmodes of the gripper are excited. Additionally, the high-speed movement of the gripper itself can induce vibrations on the wafer gripper. It should be noted that the input vibrations have a complex nature, as the wafer handler is part of a bigger lithography system. To direct the project towards a 'proof of concept', the focus of this project will be solely on dampening the first two eigenmodes of the gripper for which the assumption is made that these eigenmodes will be excited by the low-frequency disturbances.

The current solution is based on stiffening the wafer gripper close to its wrist to shift the resonance frequency of the structure beyond the frequency band of excitation. However, this only shifts the problem and this method may prove to be insufficient for the next generation gripper. Previous research has been done to investigate solution methods to increase the performance of the gripper through passive damping. Passive damping is a method to reduce the resonance peaks of the system by dissipating its vibration energy [4]. Its benefits are that the methods tend to be simple and reliable and require no control strategy. A drawback of passive damping, however, is its ineffectiveness for dampening low frequency vibrations [5]. In the research done by VDL ETG, the feasibility of passive damping methods was investigated, where they did a study on a Tuned Mass Damper (TMD) on the gripper itself, a TMD in the wrist of the gripper, Constrained Layer Damping (CLD) and any combination of the two methods. An elaboration on these solutions methods can be found in Sections 1.1.1 and 1.1.2.

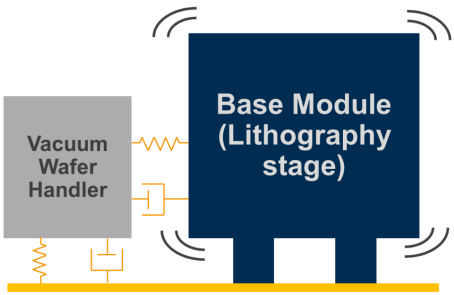

Figure 1.1: Schematic figure of the decoupled modules

1.1.1. Tuned mass damper

A TMD is a mass-spring-damper structure tuned at the eigenfrequency of the system to dissipate its vibration energy [6]. However, the thickness budget of the wafer gripper is too small to include a TMD on the gripper itself. Therefore, VDL ETG looked for possibilities to include the TMD in the wrist of the gripper, see Figure 1.2. However, this did not provide enough damping. Additionally. the robustness of the TMD solution method was very low, as the optimum for the damping of the TMD is not robust to parameter variations. If the eigenfrequencies differ slightly, the TMD needs to be re tuned. Therefore, VDL ETG concluded that the implementation of TMD for the wafer gripper is infeasible.

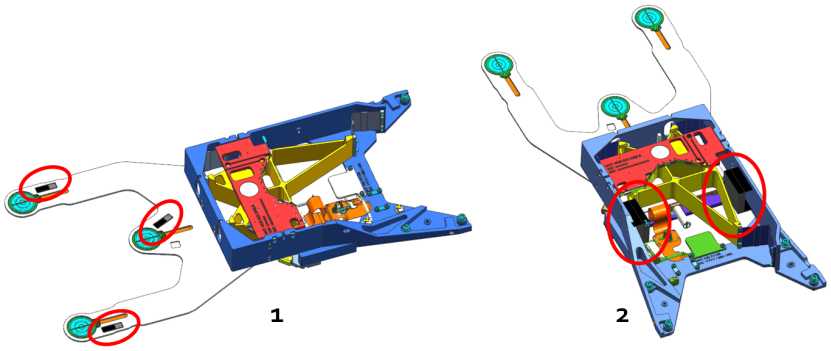

Figure 1.2: TMD implementation on wafer gripper: 1)TMD on the gripper 2)TMD in the wrist of the gripper

1.1.2. Constrained layer damping

CLD is a passive damping method where viscoelastic material layers are used to dissipate the vibration energy of the system into heat. A schematic depiction of such a structure, is provided in Figure 1.3. The viscoelastic layer is forced in shear by the stiff constraining layer when the base layer of the structure bends due to the vibrations [7]. The main benefits of CLD, like other forms of passive damping, is that no control method is required and that it is more robust when compared to a TMD. However, in the case

of the wafer gripper the stiffness decreases rapidly. This due to the tight thickness budget, which implies that material needs to be removed to replace it by this viscoelastic material. Additionally, to achieve a reasonable damping percentage, at least 35% of the gripper needs to be covered or replaced by this viscoelastic material. Properly bonding a large surface is time-and resource intensive since there is a high risk for air bubbles, and therefore this is undesirable. However, the main reason for rejection, according to VDL ETG, was that, even if possible, CLD could not provide sufficient damping of the eigenmodes. Therefore, CLD was also concluded to be infeasible.

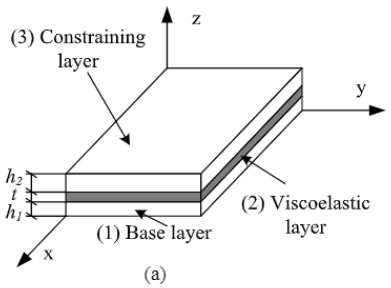

Figure 1.3: Schematic of a Constrained Layer Damping structure [7]

1.2. Key parameters of interest

To keep the research direction of the project in line with the interest of the company VDL ETG, a set of requirements have been determined. The targets are the desired goals for some of the requirements. It should be noted that these targets and requirements are no harsh goals, but rather a set of wishes from the company to keep in mind. Therefore, in this report they are referred to as 'key parameters of interest'. These parameters can be found in Table 1.1.

Table 1.1: Key parameters of interest

Key parameters of interest	**Target**	
Vacuum compatibility		
Compactness in z-direction	<2.5	mm
-Static deflection	<275	μm
Modal damping		
Low mass		
-Mass wafer	125	g
-Mass end-effector gripper	500	g
Manufacturability		
Compatibility with other components of the system		

1.3. Report outline

This report contains several chapters of which the first one is a literature review on the different damping methods that are suitable for thin structures, such as the VDL wafer gripper. Background theory on piezoelectric materials will be provided, as well as their coupling relation between the mechanical and electrical domain. This coupling relation will be used to investigate the possibilities for implementing passive damping and active damping to the structure and to design the most efficient placement of the piezoelectrics on the host structure. Furthermore, a modal analysis will be provided for a state-of-the-art wafer gripper. Based on this analysis, active damping will be implemented onto the wafer gripper where positive position feedback (PPF) will be used as a control algorithm to dampen the eigenmodes. To validate the performance of these damping methods, an experiment has been set up of which the results will be compared and discussed. Lastly, a conclusion is provided and the possibilities for future work will be discussed.

2

Literature review: damping methods for thin flexible end-effectors

Vibration suppression of flexible end-effectors has become one of the great challenges within the semiconductor industry to achieve the precision required to produce chips. This literature review presents a systematic overview of current trends in terms of dampening thin structures using smart materials. The emphasis is placed on the use of piezoelectrics, as they are best suited for the integration on thin structures. The basic principles on the electromechanical behaviour of piezoelectric materials are provided, where a back-of-the-envelope formula for the electromechanical coupling factor is provided that can be optimized for a smart structure including piezoelectric materials. The most commonly used damping methods using piezoelectrics are shunting and active vibration control. Different commonly used strategies are discussed, of which the most promising methods are compared.

2.1. Smart materials and structures

The demand for lightweight structures has been ever increasing, which leads to new challenges on vibration control technology. Lightweight and thin structures tend to be more prone to vibrations and are affected more when put under the same excitation as other structures. Smart materials, which are characterized by their coupling between different physical domains, are being researched to provide new methods to contribute to vibration attenuation [2]. These smart materials can be integrated in a so called 'smart structure', that can reduce structural vibrations through the integration of sensors, actuators and an appropriate control system [3]. The most common smart materials for the implementation in thin structures are: piezoelectric materials [8–13], shape memory alloys [14–17], thermo-elastomers [8, 18], and electro-active polymers [19, 20]. Piezoelectric materials tend to be the most common, as they are extensively used both as sensors and actuators [4], whereas the other materials tend to be less common. Shape memory alloys are materials which, within a specific temperature interval, are able to recover a predefined shape after deformation. The alloy element may exert large forces when recovering its predefined shape; making the material suitable for actuators [15]. Shape memory alloys are best used for one-way tasks, and can only be used for low frequency and low precision applications, due to the time that is needed to heat and cool the material [4, 16]. These limitations can be supported by the paper of Da Silva [21], where the use of a shape memory actuator for the vibration control of a beam was experimentally investigated to check its feasibility. The study showed that the response time was limited to 0.1Hz, and that after 0.16Hz the system was unable to track the target function due to the slow cooling speed of the actuator [21]. The same limitation holds for thermo-elastomers, which are inherently dependent on the heating and cooling of elastomers. Furthermore, electroactive polymers are polymers that can transduce electrical energy into mechanical energy. A type of electroactive polymer that can offer comparable amounts of strains to the previously mentioned smart materials are dielectric elastomers. Other types of electroactive polymers, such as piezoelectric polymers, polyelectrolyte gels and ionic polymer metal composites, typically offer low stresses or are in early stages of research [15]. Dielectric elastomer actuators have a high obtainable strain and energy density, but a general disadvantage is the high voltage that is required which is in the range of several kV [15, 20].

2.2. Piezoelectric effect

Piezoelectric materials are materials that produce an electrical charge when a mechanical stress is applied [22]. There are several categories of piezo electric materials: naturally occurring crystalline piezoelectric materials, piezoelectric ceramics, such as lead zirconate titanate (PZT)), piezoelectric composites, and piezoelectric polymers, such as polyvinylidene fluoride (PVDF) [23]. In Figure 3.1 a schematic depiction of a piezoelectric transducer, with its polarization direction (dipole alignment), is provided. Piezoelectric materials have the property that they generate a voltage when compressed along their polarization direction, or loaded in tension perpendicular to their direction of polarization. This phenomenon is called the 'direct piezoelectric effect', which is used to have the piezo electric transducer operate as a sensor (see Section 2.2.3). The inverse holds as well, where when a voltage is applied to the transducer, the piezoelectric material elongates perpendicular to the polarization direction or expands along the same direction. In this way the transducer can be used as an actuator [22]. The relationship between the applied stresses to the piezoelectric element is assumed to be linearly proportional, according to IEEE standards [24]. The same holds for the applied voltage and strain to the piezoelectric transducer. To describe the electromechanical properties of the transducer, the following constitutive equations are introduced [2, 15, 22, 24]:

$$\begin{bmatrix} D \\ S \end{bmatrix} = \begin{bmatrix} \epsilon^T & d \\ d & s^E \end{bmatrix} \begin{bmatrix} E \\ T \end{bmatrix} \tag{2.1}$$

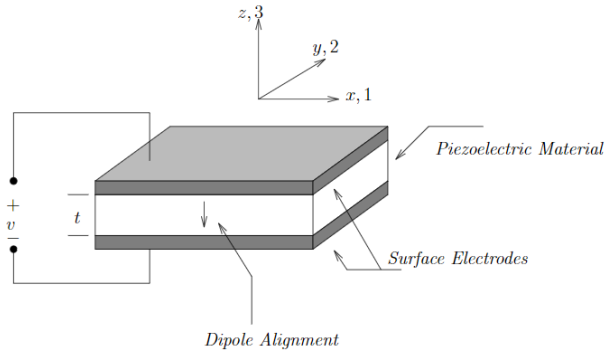

Figure 2.1: Schematic diagram of a piezoelectric transducer [22]

where $D(C/m2)$ is the electrical displacement, which is equal to the electric charge accumulated in the electrodes deposited on the surface of the piezoelectric transducer. $S(m/m)$ is the material strain of the piezoelectric transducer. $E(V/m)$ is the electric field and $T(N/m2)$ is the normal stress. $\epsilon^T(C/(V.m))$ is the electric permittivity of the material at a constant stress and $s^E(m2/N)$ is the mechanical compliance of the material. Lastly, $d(m/V)$ is the strain piezoelectric constant, which is defined as the ratio of developed free strain to the applied electric field. d is usually described with subscripts d_{ij}, that indicate the orientation of the electric field E in the i-direction, which is also the dipole alignment direction, for a strain S in the j-direction [15, 22]. Two common constants are d_{33} and d_{31}, where for d_{33} the piezoelectric material exerts a strain along the polarization direction (z-axis, 3), and for constant d_{31}, the electric field is applied along the z-axis,3 for which the piezo electric material elongates along the x-axis,1(commonly used for bending actuators).

2.2.1. Piezoelectric bending actuator

Piezoelectric bending actuators are actuators that use the inverse piezoelectric effect to extend along the longitudinal direction and as such can induce a strain distribution along a beam [22]. In Figure 2.2 a schematic depiction of such a beam is provided. The assumption is made that the transducer is 'perfectly' bonded to the beam, implying that the bonding layer is then able to completely transfer the stresses and strains [25]. A description on the influence of the bonding layer can be found in Section 2.2.4. Furthermore, it is assumed that the piezoelectric bending transducer is a rectangular patch and that the thickness of the patch is smaller than the thickness of the beam. Additionally, it is assumed

that the strain is uniform across the piezoelectric patch. In Equation 2.2 the relation between the free strain of the piezoelectric transducer ε_p and the voltage V_p is provided, which is also dependent on the thickness $t_p(m)$ of the transducer and the strain piezoelectric constant d_{31} [22].

$$\varepsilon_p = \frac{d_{31}}{t_p V_p} \tag{2.2}$$

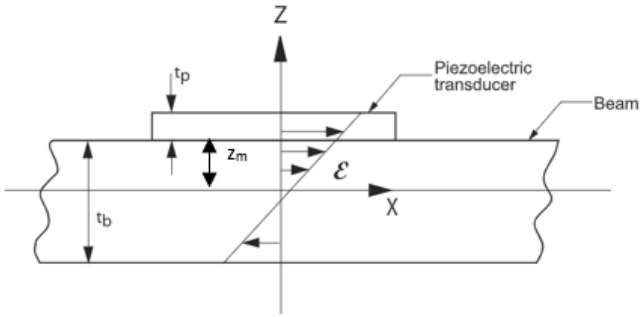

Figure 2.2: Schematic depiction of a beam with a piezoelectric bending transducer [22]

2.2.2. Electromechanical coupling

In this section, the constitutive equations from Equation 2.1 are used to derive the relations between the input piezoelectric voltage to the charge, elongation of the bending actuator, and the force that can be exerted by the transducer. Equation 3.3, shows the electromechanical coupling coefficient k_{31}^2 .

$$k_{31}^2 = \frac{d_{31}^2}{s^E \epsilon^T} \tag{2.3}$$

This coefficient indicates the efficiency of the conversion of mechanical energy into electrical energy, and vice versa [2, 4, 22]. This coefficient is used when modelling the behaviour of piezoelectric transducers to be able to determine the capability of piezoelectric transducers to convert mechanical vibration energy of the host structure into electrical energy, which will be discussed in Section 2.3. Typical values for k_{31}^2 are between 0.3-0.7 [4]. Equation 2.1 can be rewritten in the form as shown in Equation 2.4.

$$\begin{bmatrix} D \\ T \end{bmatrix} = \begin{bmatrix} \epsilon^T(1-k_{31}^2) & \frac{d_{31}}{s^E} \\ -\frac{d_{31}}{s^E} & \frac{1}{s^E} \end{bmatrix} \begin{bmatrix} E \\ S \end{bmatrix} \tag{2.4}$$

By integrating Equation 2.4 over the volume over the transducer, Equation 2.7 can be obtained using the following relations: $Q = AD$ (the total electric charge on the electrode of the transducer); where $A(m)$ is the area of the transducer, $E = V_p/t_p$ (electric field); $F = AT$ (total force); $C_p = (\epsilon^T A)/t_p$ (capacitance of the transducer), where $l(m)$ is the length of the piezoelectric transducer, $\Delta = Sl$ (total extension) [4].

$$\int_V D dV = \int_V \epsilon^T \left(1-k_{31}^2\right) E dV + \int_V \frac{d_{31}}{s^E} dV \tag{2.5}$$

$$\int_V T dV = -\int_V \frac{d_{31}}{s^E} E dV + \int_V \frac{1}{s^E} S dV \tag{2.6}$$

$K_{ss} = \frac{A}{s^E l}$ is the stiffness with short-circuited electrodes [4]. Short-circuited implies that the two electrodes on the piezoelectric transducer are connected externally with an ideal wire ($R = 0$ and $\Delta V = 0$) [26].

$$\begin{bmatrix} Q \\ F \end{bmatrix} = \begin{bmatrix} C_p(1-k_{31}^2) & d_{31}K_{ss} \\ -d_{31}K_{ss} & K_{ss} \end{bmatrix} \begin{bmatrix} V_p \\ \Delta \end{bmatrix} \tag{2.7}$$

Inverting Equation 2.7, then gives

$$\begin{bmatrix} V_p \\ F \end{bmatrix} = \frac{K_{ss}}{C_p(1-\kappa_{31}^2)} \begin{bmatrix} K_{ss} & -d_{31} \\ -d_{31} & K_{ss} \end{bmatrix} \begin{bmatrix} Q \\ \Delta \end{bmatrix} \tag{2.8}$$

Admittance of a beam with a piezoelectric bending transducer

Admittance is defined as the charge over voltage and indicates the amount of current that can flow through a system. It is the inverse of the impedance, where the impedance is the characteristic of an electrical circuit to oppose current flow [27]. The admittance can be used to get an expression for the electromechanical coupling of the piezoelectric transducer that is attached to a host structure, which in this case is the beam as shown in Figure 2.2. To obtain the relation between the charge and voltage, the second constitutive equation as shown in Equation 2.9 is used. Since D is the electrical displacement in $(C/m2)$, integrating D over the area of the electrode will give the electrical charge.

$$D = \epsilon^T \left(1-\kappa_{31}^2\right) E + \frac{d_{31}}{s^E} S \tag{2.9}$$

$$Q = \int_A D dA = \int_A \epsilon^T \left(1-\kappa_{31}^2\right) E dA + \int_A \frac{d_{31}}{s^E} S dA \tag{2.10}$$

The material strain of the piezoelectric transducer $S\ (m/m)$ can be expressed as $S = -z_m w''$ [4], where z_m is the distance to the mid-axis of the beam, as indicated in Figure 2.2 and w is the displacement at the tip of the beam, for which the expression is shown in Equation 2.11 [[4], eq.(4.64, 4.65)]. z_i is the modal amplitude and $\phi_i(x)$ are the mode shapes. The displacement at the tip of the beam can then be expressed as the summation of the modal amplitudes for each mode shape, as shown in Equation 2.11 [[4], eq.(4.64, 4.65)].

$$w = \sum_{i=1}^{n} z_i \phi_i(x) = -\frac{d_{31}}{s^E} b_p z_m V_p \sum_{i=1}^{n} \frac{\Delta\theta_i \phi_i(x)}{\mu_i (s^2+\omega_i^2)} \tag{2.11}$$

where μ_i is the modal mass of the host structure, and ω_i^2 is the natural frequency. $\Delta\theta_i = \phi'(x_1) - \phi'(x_2)$ is the difference of the spatial derivative of mode i at the ends of the piezoelectric patch. Filling in for S and using the voltage relation for the electric field E gives:

$$Q = \int_A \epsilon^T \left(1-\kappa_{31}^2\right) \frac{V}{t}\, dA + \int_A \frac{d_{31}}{s^E} (-z_m w'')\, dA \tag{2.12}$$

$$Q = \int_A \epsilon^T \left(1-\kappa_{31}^2\right) \frac{V}{t}\, dA + \frac{d_{31}}{s^E} z_m b_p \int_{x_1}^{x_2} w'' dx = \left(1-\kappa_{31}^2\right) C_p V_p - \frac{d_{31}}{s^E} z_m b_p [w'(x_2) - w'(x_1)] \tag{2.13}$$

Filling in for the displacement w, and using the geometrical expression for the capacitance and Equation 3.3 results in:

$$\frac{Q}{\left(1-\kappa_{31}^2\right) C_p V_p} = 1 + \frac{\kappa_{31}}{(1-\kappa_{31}^2)} \sum_{i=1}^{n} \frac{1}{1+s^2/\omega_i^2} \frac{b_p t_p z_m^2 \Delta\theta_i^2}{s^E l \mu_i \omega_i^2} \tag{2.14}$$

$$\frac{Q}{V} = C_p \left(1-\kappa_{31}^2\right) \left[1 + \sum_{i=1}^{n} \frac{K_i^2}{1+s^2/\omega_i^2}\right] \tag{2.15}$$

which is the frequency response function for the admittance, or equivalently the dynamic capacitance of the beam with the piezoelectric bending transducer attached, where K_i^2 is expressed as follows [[4], eq.(4.74, 4.76, 4.77)]:

$$K_i^2 = \frac{\kappa_{31}^2}{\left(1-\kappa_{31}^2\right)} \frac{\Delta\theta_i^2}{\mu_i \omega_i^2} \frac{E_p b_p t_p z_m^2}{l} \cong \frac{\Omega_i^2 - \omega_i^2}{\omega_i^2} \tag{2.16}$$

where Ω_i^2 is the natural frequency for open electrodes and E_p is the Young's modulus. It can be noted that the electromechanical coupling factor K_i^2 is dependent on parameters which can be determined analytically and experimentally, which is useful to validate the experimental values for K_i^2. Furthermore, Equation 2.16 can serve as a back of the envelope method for determining an optimal design for piezoelectric bending patches on a host structure.

2.2.3. Piezoelectric sensing

Piezoelectric transducers are also suitable to be used as sensors and are most commonly used for measuring low strain levels [22]. The relation between the voltage generated by the transducer and the strain exerted, can be derived by rewriting the relation for the capacitance, as shown in Equation 2.17 [[27], eq.(5.2)].

$$V_p = \frac{Q}{C_p} \tag{2.17}$$

The charge Q can be found through integrating the second constitutive equation over the area of the transducer, as done in Equation 2.10. Assuming that there is no electric field induced on the transducer $(E = 0)$, and the strain is along one direction (x-axis,1), the following expression can be obtained.

$$Q = \frac{d_{31}\ b_p}{s^E} \int_l \varepsilon_1 dx \tag{2.18}$$

Filling in for the charge, the relation between the voltage and strain can be acquired, as shown in Equation 2.19.

$$V_p = \frac{d_{31}\ b_p}{s^E C_p} \int_l \varepsilon_1 dx = \frac{d_{31} E_p b_p}{C_p} \int_l \varepsilon_1 dx \tag{2.19}$$

2.2.4. Influence of bonding

Piezoelectric transducers need to be bonded to their host structure, where this bonding layer contributes to the dynamic behaviour of the structure. This is usually done by bonding the piezoelectric transducer to the host structure with a (conductive) epoxy [28]. Several studies have been conducted that study the effect of these bonding layers for piezoelectric structures, such as in the paper of Han et al. [28] where a theoretical study on the dynamical behaviour of surface-bonded piezoelectric sensors was performed. Numerical simulations showed that for high frequency cases, the strain distribution along a piezoelectric sensor becomes unpredictable due to a decrease in the bonding layer stiffness. However, for low frequency cases the strain distribution along the sensor is only influenced by the thickness of the bonding layer. Another numerical study was performed in the paper of Tinoco et al [29] to understand the effects of the adhesive layer on the electromechanical coupling of piezoelectric transducers bonded to a structure. In the papers of Bhalla et al [25] and Pietrzakowski [30], analytical models on the electromechanical coupling of a piezoelectric structure are provided that include the effects of this bonding layer. These models could be used for when the dynamics of the bonding layer contribute significantly to the dynamics of the system. For example, when the bonding layer has a relatively large thickness or the structure operates at high frequencies.

2.3. Piezoelectric shunting

Piezoelectric shunting is a passive damping method where a shunting circuit is used to provide electrical damping to a structure. No control strategy is required to dampen the modes of the system and the circuits are tuned such that they reduce the modal peaks at resonance. Furthermore, no power supply is required to drive the piezo transducers which consequently cannot cause instability of the system [31]. There are several types of shunt circuits, but generally they serve the purpose to dampen either one single mode or multiple modes in the system, of which the methods will be discussed in Section 2.3.1 and Section 2.3.2, respectively. However, this passive shunting method does have its unavoidable practical constraints giving incentive to new developments of the circuits by including active components [2]. In Section 2.3.3 an overview will be provided of the (semi-) active shunting methods.

2.3.1. Single-mode shunt circuits

There are generally two types of single-mode shunts circuits: resistive and resonant shunts. Resistive shunts are first-order circuits that include only a resistor, where the electrical energy is dissipated in the form of heat. The shunt behaves similar to a light viscoelastic damper and therefore offers very little mechanical damping [32, 33]. Resonant shunt circuits are circuits that are built up of a resistance and an inductor to tune the resonance of the electrical circuit equal to that of the mechanical system. Consequently, the circuit is in resonance and behaves like a vibration absorber [32]. Similar to mechanical vibration absorbers, shunt circuits are sensitive to changes in the natural frequency of the host structure and need to be tuned properly. In the paper of Andreaus [34], the effect of electrical parameter variations on the performance of a resonant shunting circuit was studied. Changes in the resistance values had little influence on the damping capabilities of the shunt circuit. However, uncertainties on the inductance influence the damping capabilities significantly. The paper provides equations for which design tolerances for the resistance and inductor values can be established [34]. For single-mode vibration damping, the resonant circuits are configured such that they are either in parallel or in series. Both circuits have a close to similar performance, but parallel circuits have the slight advantage that they tend to be less sensitive for finding the optimal resistance, and are therefore said to be easier to tune [2, 33, 35]. Several methods have been studied for finding the optimal resistance and inductance for a shunting circuit. Equation 2.20and Equation 2.21 provide tuning equations for an in-series circuit as first derived by Hagood et al [33].

$$L = \frac{1}{\omega_i^2 C_p \sqrt{1 + K_i^2}} \tag{2.20}$$

$$R = \frac{1}{C_p} \sqrt{\frac{K_i^2}{1 + K_i^2}} \tag{2.21}$$

It should be noted that the inductance is proportional to the inverse of the natural frequency squared and thus increases for lower frequencies. This can pose as a practical limitation for implementing a suitable inductor. In Section 2.3.3 alternative methods are discussed to solve this problem. For parallel circuits tuning equations were first proposed by Wu et al [35], where the tuning depends on the electrical resonance frequency. Other tuning methods can be found in the paper of Yan et al [32] , that provides an extensive review of the different tuning methods available. To see whether or not resistive shunting or resonant shunting can provide the required amount of damping: $\zeta_{\max_R} = \frac{K_i^2}{4}$; $\zeta_{\max_R L} = \frac{K_i}{2}$ can be used to derive the maximal damping percentage, respectively [4].

2.3.2. Multi-mode shunt circuits

Multi-mode shunt circuits are designed such that they can dampen multiple modes using the same piezoelectric transducer. Typically, there are four types of different shunt circuits used for multi-modal damping: Hollkamp shunt [36], current-blocking shunt [37], current-flowing shunt [38], and series-parallel shunt [2]. In Figure 2.3 the configurations of the circuits are schematically depicted. Hollkamp circuits have been one of the first successful attempts to dampen multiple modes through shunting. However, they are difficult to tune, since tuning one electrical resonance to suppress one specific mode will detune the rest of the shunt [32, 36]. Current-blocking shunt circuit have the main drawback that the size of the circuit can increase rapidly for the number of target modes [2, 37].

Behrens et al [38] introduced a method for which the electrical components in each branch is easier to tune, since they can be regarded as independent from each other. This method referred to as the current flowing shunt circuit and serves as an effective stable method to dampen multiple modes [38]. Lastly, there is the series-parallel shunt circuit which can also passively dampen multiple modes using one transducer, however, it offers no great advantage over the other techniques [32].

2.3.3. Active shunt circuits

Due to the practical limitations and limited robustness of passive shunt circuits, the need for active solutions grows. Active shunt circuits tend to have higher damping capabilities, but are dependent on an external power supply [22]. Therefore, stability of the system is not guaranteed. However, by

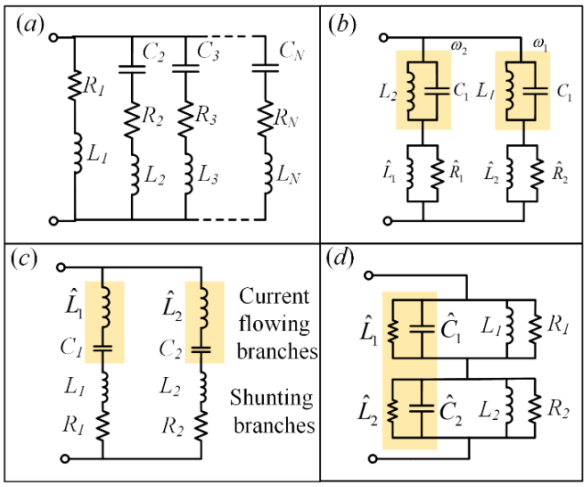

Figure 2.3: Different configurations of multi-modal shunts: A)Hollkamp shunt B)Current-blocking shunt C)Current-flowing shunt D)Series-parallel shunt [32]

including active components, such as switches, virtual inductances, and/or operational amplifiers, the shunt circuits could be augmented such that they meet system requirements.

Virtual shunt circuits
A common practical limitation for shunt circuits is that they require large inductors for when the circuit needs to be tuned at low frequencies. Typical inductor values in the low frequency band are in the magnitude of several hundreds of Henrys [39]. A solution to this would be to implement a so called virtual inductor. This type of inductor is composed out of several active and passive elements, such as operational amplifiers and resistors, to achieve high inductance values [2]. There are two types of synthetic inductors: Antoniou inductors [40] and Riordan Gyrators [41], of which Antoniou inductors are most commonly used [2]. The main advantages of these virtual inductances are that they enable the implementation of resonant shunt circuits for low frequency modes. However, they tend to be difficult to tune and are sensitive to temperature changes and/or other non-ideal conditions [22]. Additionally, the layout for virtual inductors tend to be complex and they require high-voltages.

Nonlinear shunt circuits
Another method to eliminate the need for large impractical inductors is by introducing nonlinearity to the shunt circuits. A technique that is commonly used, is synchronized switch damping (SSD) where the voltage in the piezoelectric transducer is inverted synchronously to the motion of the host structure [2]. These shunt circuits usually contain either a capacitor, resistor, or an inductor [22]. In the paper of Claude et al [42] a SSD technique is proposed that uses an inductor in the circuit to discharge the piezoelectric transducer when the circuit is in short-circuit. When the circuit is closed, the piezoelectric transducer is kept in a high-stiffness state, storing the vibration energy, after which the circuit is switched to an open circuit (low-stiffness state) to dissipate the energy [2, 43]. A drawback to these nonlinear shunt circuits is that the switching in the circuit can also influence the dynamics of the system at other frequencies. This could excite higher order modes in the system, which is generally undesirable.

Adaptive shunt circuits
Adaptive shunt circuits are resonant shunts that are augmented by adding sensors to the system, that serve as input for, a so called, adaptation law [32].This ensures that the shunt circuit becomes more robust to parameter variations, even when the circuit is severely detuned [44]. In Figure 2.4 a schematic overview is provided of the layout of such an adaptive shunt circuit.

Several layouts and adaptation laws have been researched for their effectiveness. In the papers of Niederberger et al [45] and Gripp et al [46] an adaptation law is proposed that is based on minimizing the relative phase difference between the velocity of the host structure and the current flowing through the circuit. An online adaptive circuit is discussed in the paper of Fleming et al [44], where

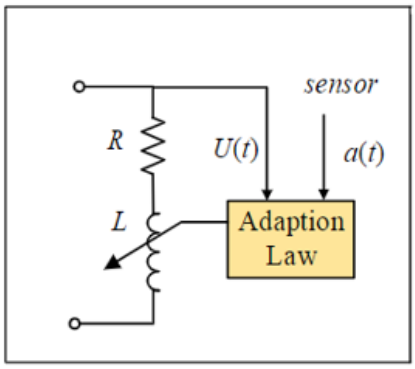

Figure 2.4: Layout of an adaptive shunt circuit [32]

a virtual impedance is used along with time-varying transfer functions to change the tuning parameters of the shunt in real time. The main advantage of these adaptive circuit is their ability to make the shunts more robust, however, by adding different active components to the system a power supply is required. Moreover, by introducing sensors to the circuit and implementing this adaptation law, there is little design advantage gained when compared with the active vibration control strategies that will be discussed in Section 2.4.

2.4. Active vibration control

Piezoelectric transducers can also be used to dampen vibrations by active means, through the implementation of an appropriate control strategy. In this section the most commonly used control strategies to dampen thin structures using piezoelectrics will be discussed: direct velocity feedback (DVF), integral force feedback (IFF), and positive position feedback (PPF). These control strategies are such that they require relatively little control effort. Moreover, they tend to be easily implementable since they require little knowledge of the system, which is important for the realization of smart structures as their mechanical design can become complex [4]. It should be noted that the strategies discussed in this section are based on collocated systems, meaning that the sensors and actuators are placed at the same location on the host structure. This ensures stability for a large range of control systems.

2.4.1. DVF

Direct velocity feedback uses the output of a velocity sensor to provide feedback to the system. The output signal from the velocity sensors are multiplied by an appropriate gain, after which the signal is fed back to the force input of the system. In this case this force input can be provided by piezoelectric bending transducers attached to the host structure. In the paper of Wang et al [47], practical guidelines are provided for tuning the gain feedback whilst considering the damping performance. The maximum modal damping that can be achieved through DVF can be determined through Equation (16) [4, 48].

$$\zeta_{max} \cong \frac{\omega_i - z_i}{2z_i} \tag{2.22}$$

This approximation on the damping performance only holds for when the value of the modal amplitude z_i is larger than one-third of the natural frequency ω_i [4]. It should be noted that DVF does require control effort at all frequencies, which could result in a reduced efficiency of the system [4].

2.4.2. IFF

Integral force feedback uses a force sensor to obtain a force output signal that is multiplied with a gain and an integrator before being fed back to the force input of the system [4]. The main advantage of this control strategy is it simplicity, stability and robustness, similar to DVF. However, by using an integrator with a gain, control effort is required for frequencies other than the targeted resonance frequencies. In the paper of Teo et al [48], a classical, as well as an optimal tuning method is provided for the tuning of the IFF controller. The maximum achievable damping using IFF can be computed the same way as

for DVF, by using Equation 2.22 [48].

2.4.3. PPF

Positive position feedback is a control strategy that introduces a second-order low pass filter tuned to a specific resonance frequency [4]. PPF is a commonly used control strategy when using piezoelectric transducers to effectively dampen specific modes in the system, without destabilizing other modes [49]. The second-order low pass filter for PPF control is provided in Equation 2.23 [4]. This filter needs to be such that the filter frequency ω_f is tuned to the resonance frequency of the host structure. The gain g and damping ratio ζ_f should be tuned accordingly to achieve the desired damping performance.

$$H(s) = -\frac{g}{s^2 + 2\zeta_f \omega_f s + \omega_f^2} \tag{2.23}$$

Since the filter is based on this tuning, a slight shift in eigenfrequencies of the structure could result in detuning of the filter. When the PPF controller is detuned, the damping performance decreases and therefore this method has limited robustness when it comes to parameter variations. These parameter variations could be caused by temperature differences, design changes, and changes in the stiffness of the host structure, for example. However, PPF only requires control effort on the targeted modes, which increases the efficiency of the system. To simultaneously dampen multiple modes in the system, PPF filters can also be used in parallel where each filter is tuned to one specific mode [4].

2.5. Conclusion

This literature review provides an overview for the current trends in terms of dampening thin structures using smart materials to enable a high degree of integration. The state-of-the-art has been investigated and provided, for which the most promising and well researched methods have been elaborated on. Piezoelectric materials tend to be the best suited for dampening thin structure, when looking at the current developments in smart materials. For the integration of piezoelectric materials onto a host structure, the electromechanical coupling is of importance. Derivations on the admittance of the piezoelectric transducer have been provided to obtain a back-of-the envelope expression for the effective electromechanical coupling factor. This coupling factor relates to the maximum achievable modal damping, since it shows the measure of how much mechanical vibration energy can be converted into electrical energy, and vice versa. The higher this coupling factor the more damping can be achieved. Shunting and active vibration control are proposed damping methods that could be implemented to provide modal damping to a thin structure. For single-mode shunting the best method for dampening the eigenmodes are through the use of resonant shunt circuits, for which parallel shunts are said to be easier to tune. However, these circuits tend to use high inductance values which poses as a practical limitation. Through the addition of active components the practical implementation can be achieved, at the expense of the circuit's complexity and power supply. Therefore, it could be more beneficial to switch to active vibration control. DVF and IFF are robust, simple and stable control strategies, but they lack in efficiency. Whereas PPF controllers are more suited to dampen specific target modes to increase the system's efficiency, but are limited in their robustness.

3

Vibration suppression of a state-of-the-art wafer gripper

In this chapter the main work of the project will be presented, where active vibration control will be applied to a state-of-the-art wafer gripper to satisfy the objective of achieving at least 5% modal damping. A short summary of the relevant results from the literature review will be provided, after which the design choices for the damped system will be explained. The electromechanical coupling factor is used as a back-of-the-envelope method for the design process. An experimental setup has been built to check the modal behaviour for the gripper to design an appropriate system and to select the eigenmodes that need to be targeted. The same setup is then used to check the performance of the active setup, after which the results are discussed to draw a conclusion on the achieved performance.

3.1. Piezoelectric effect

Piezoelectric materials are materials that produce an electrical charge when a mechanical stress is applied [22]. In Figure 3.1 a schematic depiction of a piezoelectric transducer, with its polarization direction (dipole alignment), is provided. Piezoelectric materials have the property that they generate a voltage when compressed along their polarization direction, or loaded in tension perpendicular to their direction of polarization. This phenomenon is called the 'direct piezoelectric effect', which is usually used to have the piezoelectric operate as a sensor. The inverse holds as well, where when a voltage is applied to the transducer, the piezoelectric material elongates perpendicular to the polarization direction or expands along the same direction. In this way the transducer can be used as an actuator [22]. The relationship between the applied stress to the piezoelectric element is assumed to be linearly proportional, according to IEEE standards [24]. The same holds for the applied voltage and strain to the piezoelectric transducer. To describe the electromechanical properties of the transducer, the following constitutive equations are introduced [2, 15, 22, 24, 50]:

$$\begin{bmatrix} D \\ S \end{bmatrix} = \begin{bmatrix} \epsilon^T & d \\ d & s^E \end{bmatrix} \begin{bmatrix} E \\ T \end{bmatrix} \tag{3.1}$$

where $D(C/m^2)$ is the electrical displacement, which is equal to the electric charge accumulated in the electrodes deposited on the surface of the piezoelectric transducer. $S(m/m)$ is the material strain of the piezoelectric transducer. $E(V/m)$ is the electric field and $T(N/m2)$ is the normal stress. $\epsilon^T(C/(V.m))$ is the electric permittivity of the material at a constant stress and $s^E(m^2/N)$ is the mechanical compliance of the material. Lastly, $d(m/V)$ is the strain piezoelectric constant, which is defined as the ratio of developed free strain to the applied electric field. d is usually described with subscripts d_{ij}, that indicate the orientation of the electric field E in the i-direction, which is also the dipole alignment direction, for a strain S in the j-direction [15, 22].

There are several categories of piezo electric materials: naturally occurring crystalline piezoelectric materials, piezoelectric ceramics, such as lead zirconate titanate (PZT)), piezoelectric composites, and piezoelectric polymers, such as polyvinylidene fluoride (PVDF) [23]. PZT and PVDF are the most

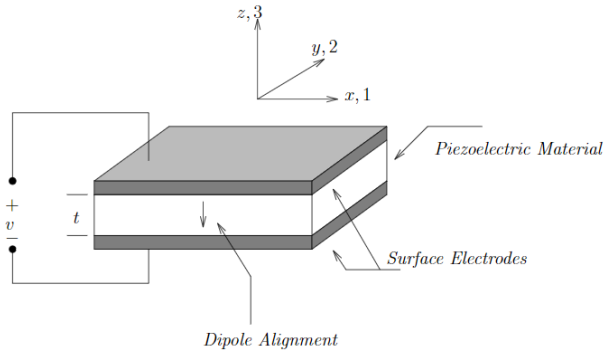

Figure 3.1: Schematic diagram of a piezoelectric transducer [22]

common types of materials, where PZT transducers are known for their high stiffness and PVDF transducers for their flexibility.

3.1.1. Electromechanical coupling factor

The electromechanical coupling factor serves as a measure to show the efficiency for which the mechanical energy is converted to electrical energy, and vice versa. This measure can be used to determine how and where to implement piezoelectrics onto a host structure. The effective coupling between a piezoelectric transducer and its host structure, in the case a wafer gripper, can be determined through the use of Equation 3.2 [4]. The value for the coupling factor tends to be found experimentally by measuring the natural frequency of the structure for open-circuited electrodes $\Omega_i(rad/s)$ and short-circuited electrodes $\omega_i(rad/s)$. However, it can also be determined analytically through the admittance of a piezoelectric transducer that is 'perfectly' attached to its host structure. This means that the influence of the bonding layer between the structure and the piezoelectric transducer is left out of scope. It is assumed that admittance here is defined as the charge over voltage and indicates the amount of current that can flow through the system [27]. Another assumption is that the host structure behaves like a beam and that the piezoelectric transducer is much thinner than the thickness of the host structure.

$$K_i^2 = \frac{\kappa_{31}^2}{1-\kappa_{31}^2}\frac{\Delta\theta_i^2}{\mu_i\omega_i^2}\frac{E_p b_p t_p z_m^2}{l} \cong \frac{\Omega_i^2-\omega_i^2}{\omega_i^2} \tag{3.2}$$

Equation 3.2 can be divided into three parts, where the first fraction is composed solely of material parameters of the piezoelectric transducer, namely κ_{31}^2. κ_{31}^2 is the electromechanical coupling factor of the piezoelectric material, which can be determined using Equation 3.3.

$$\kappa_{31}^2 = \frac{d_{31}^2}{s^E \epsilon^T} \tag{3.3}$$

The second fraction depends on the modal behavior of the host structure, where $\Delta\theta_i^2$ is the difference of the slope of the mode shapes of the host structure at the beginning and end of the piezoelectric patch, μ_i is the modal mass of the host structure, and $\omega_i^2(rad/s)$ is its eigenfrequency. The third fraction are design parameters for the selected piezoelectric transducer, where $E_p(Pa)$ is the Young's Modulus of the material, $b_p(m)$ is the width of the piezoelectric patch, $t_p(m)$ is the thickness, $z_m(m)$ is the distance from the piezoelectric patch to the mid-axis of the host structure, and $l(m)$ is the length of the piezoelectric transducer [4]. It can be noted that the electromechanical coupling factor K_i^2 is dependent on parameters which can be determined analytically and experimentally, which is useful to validate the experimental values for K_i^2. Furthermore, Equation 3.2 can serve as a back of the envelope method for determining an optimal design for piezoelectric bending patches on a host structure. Moreover, this coupling factor relates to the maximum achievable modal damping, since it shows the measure of how much mechanical vibration energy can be converted into electrical energy, and vice versa. The higher the coupling factor, the more damping can be achieved.

3.1.2. Piezoelectric shunting

Piezoelectrics can be used both in passive damping and active damping methods. Passive damping can be performed through the use of shunting. A shunt circuit is then used to provide electrical damping to the host structure. The main advantage of shunting is that no control strategy or power supply is required, which consequently can not cause instability of the system [31]. There are several types of shunt circuits but generally they serve the purpose to dampen either one single mode or multiple modes in the system. For single mode shunts, there are two types: resistive shunt circuits and resonant shunt circuits. Resistive shunts are first-order circuits that include a only a resistor, where the electrical energy is dissipated in the form of heat. The shunt behaves similar to a light viscoelastic damper and therefore offers very little mechanical damping [32, 33]. Resonant shunts are circuits that are built up of a resistance and an inductor to tune the resonance of the electrical circuit equal to that of the mechanical system. Consequently, the circuit is in resonance and behaves like a vibration absorber [32]. Similar to mechanical vibration absorbers, shunt circuits are sensitive to changes in the natural frequency of the host structure and need to be tuned properly. The maximum achievable modal damping that can be achieved for these single mode shunts are determined by using the coupling factor. In Equation 3.4 and 3.5 the relation between the coupling factor and the theoretical maximum achievable damping is provided for resistive and resonant shunts, respectively [4].

$$\zeta_{max_R} = \frac{K_i^2}{4} \tag{3.4}$$

$$\zeta_{max_{RL}} = \frac{K_i}{2} \tag{3.5}$$

Multi-mode shunts can be used to dampen multiple modes in the system using the same piezoelectric transducer. Typically, there are four types of different shunt circuits used for multimodal damping: Hollkamp shunt [36], current-blocking shunt [37], current-flowing shunt [51], and series-parallel shunt [2]. All four shunts have similar damping characteristics, but different tuning methods based on the application. A common practical limitation for shunt circuits is that they require large inductors for when the circuit needs to be tuned at low frequencies. Typical inductor values in the low frequency band are in the magnitude of several hundreds of Henrys [39].

3.1.3. Active vibration control

Piezoelectric transducers can also be used to dampen vibrations by active means, through the implementation of an appropriate control strategy. The most commonly used control strategies to dampen thin structures using piezoelectrics are: direct velocity feedback (DVF), integral force feedback (IFF), and positive position feedback (PPF). These control strategies are such that they require relatively little control effort. Moreover, they tend to be easily implementable since they require little knowledge of the system, which is important for the realization of smart structures as their mechanical design can become complex [4]. It should be noted that the strategies discussed in this section are based on collocated systems, meaning that the sensors and actuators are placed at the same location on the host structure. This ensures stability for a large range of control systems. DVF uses the output of a velocity sensor to provide a gain feedback to the system, where IFF uses a force sensor to obtain a force output signal that is multiplied with a gain and an integrator before being fed back to the force input of the system [4]. DVF and IFF have in common that they require control effort at all frequencies, which could reduce the efficiency of the system [4]. However, PPF control feeds back a second-order low pass filter tuned to a specific resonance frequency. Therefore, PPF only needs control effort on the targeted modes, which increases the efficiency of the system. To simultaneously dampen multiple modes in the system, PPF filters can also be used in parallel where each filter is tuned to one specific mode [4]. PPF is a commonly used control strategy when using piezoelectric transducers to effectively dampen specific modes in the system, without destabilizing other modes [49]. A drawback of PPF, however, is its limited robustness. A slight shift in eigenfrequencies of the structure could result in detuning of the filter.

3.1.4. Comparison of different damping methods

The state-of-the-art has been investigated and smart structures are investigated in order to explore the possibilities to dampen thin end-effectors. For the implementation of piezoelectric materials onto a host

structure, the electromechanical coupling is of importance. Shunting and active vibration control are proposed damping methods that could be implemented to provide modal damping to a thin structure. However, for shunting the limitation is that the circuits tend to use high inductance values for low frequencies, which poses as a practical limitation. Circuits that do not use an inductor tend to have limited damping capabilities [32]. It should still be noted that shunting has considerable advantages and is a worthwhile method to explore in the future. For the wafer gripper, however, the choice was made to perform active vibration control.

3.2. Design of a damped flexible end-effector

3.2.1. Selection of piezoelectric transducers

In order to allow for a proper implementation of the piezoelectric transducer onto the wafer gripper, the type of actuator needs to be selected. Assuming a 'perfect' bonding layer, Equation 3.2 is used to choose the piezoelectric bending actuator such that the coupling between the transducer and host structure is optimal. The material chosen for the piezoelectric transducer in this case is PZT, because of its high stiffness [4]. A larger Young's modulus E_p means a higher value for the coupling factor, based on the relation provided in Equation 3.2. Additionally, PZT transducers can exert larger forces on the structure than PVDF, which is favorable since the wafer gripper is made of a stiff ceramic material that has a Young's modulus of 350 GPa. Furthermore, from Equation 3.2 there can be seen that for large widths and thicknesses of the piezoelectric patch the value for the coupling factor increases. Therefore, the width is taken to be the width of the fingers of the wafer gripper. Looking at the commercial availability of piezoelectric patches, the maximum thickness that can be produced is 0.8mm. It should be noted that the slope of the modes shapes is dependent on the placement of the piezoelectrics on the gripper.

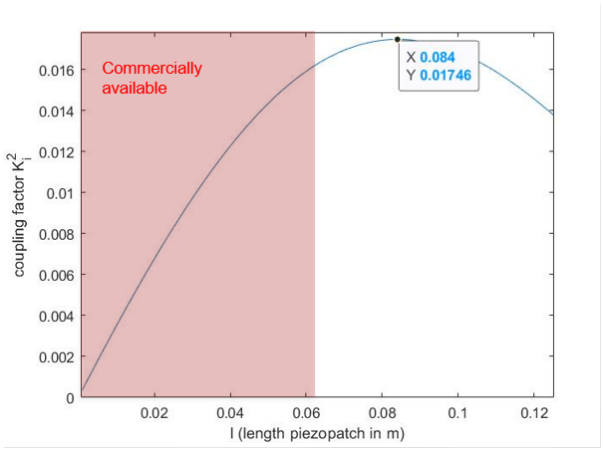

Figure 3.2: Optimization for piezo patch size based on coupling factor

This is in turn dependent on the length of the piezoelectric transducers. In Figure 3.2 the relation between the coupling factor and the length of the piezoelectric transducer is depicted for a PZT patch with a thickness of 0.8 mm and the width set to the width of the fingers of the wafer gripper. From the figure it can be seen that the optimal patch should have a length of 84 mm, however, the largest commercially available patches have a length of 61 mm. The patches that will be used for actuation are the P-876.A15 DuraAct Patch Transducers from Physik Instrumente (PI). Two patches will be used for each of the fingers of the wafer gripper. For the sensing patches the P-876.SP1 DuraAct Patch Transducers from Physik Instrumente (PI) are used, because of their small dimensions and their compatibility with the actuators, as they produce the same strain to voltage output. These sensor patches should be as small as possible to contribute as little as possible to the stiffness of the wafer gripper, in order to limit the change in dynamics. The coupling factor does not have to be optimized for the sensors, because it is solely used for measuring the strain at one specific location and the priority is set to limit the changes in dynamics of the wafer gripper. The influence of the piezoelectrics on the dynamics of the host structure will be investigated in Section 3.3.4.

3.2.2. Control algorithm

In Figure 3.3, a schematic overview of the control loop is provided. From the control algorithms mentioned in Section 3.1.3, PPF will be used to effectively dampen the eigenmodes of the wafer gripper due to its effectiveness and limited control effort. This control strategy introduces one or several tuned second-order low pass filters to dampen the system. In Figure 3.3, $G(s)$ is the transfer function of the plant, d is a disturbance that is acting on the wafer gripper, and y is the position output. For the PPF algorithm, the second-order low pass filter is multiplied with a negative gain. This gain can be tuned to achieve the desired amount of damping. It should be noted that the value for the gain determines the stability of the system, since if the gain is set too high, the system can become unstable or the actuator can saturate. However, the instability tends to occur for large gains where the static loop gain is larger than 1, see the condition in Equation 3.6.

$$gG(0) < 1 \tag{3.6}$$

These high gains are usually not used in practice [4]. The remaining parameters that need to be tuned are: ζ_f and $w_f(rad/s)$, which are the damping and filter frequency, respectively.

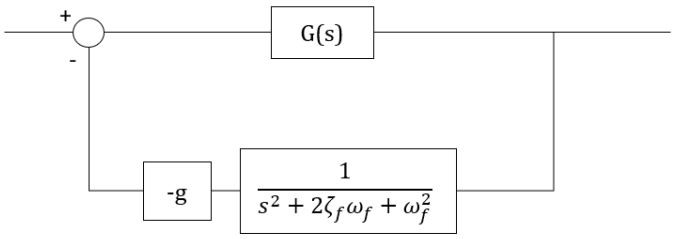

Figure 3.3: Diagram of the control loop

The performance of the PPF controller is mostly reliant on the filter frequency, which should be set equal to the resonance frequency of the structure. The damping ratio influences the robustness of the PPF controller making the algorithm less robust for lower values of the damping ratio, and vice versa.

3.3. Method

In this section, the method used for the implementation of piezoelectric transducers onto a state-of-the-art wafer gripper will be discussed. Several aspects have to be determined in order to design a system that is effectively dampened to achieve at least 5% modal damping. The placement of the piezoelectric patches will be determined through the relation of the coupling factor and modal analysis data. This data will be acquired through the use of a Polytec Scanning Doppler Vibrometer PSV-400 that will scan the surface of the gripper to measure the actual mode shapes for the resonance frequencies of the gripper. The experimental setup used for the acquisition of the modal analysis data will be further described in Section 3.3.1. After having determined the placement of the piezoelectric transducers, several tests will be performed to investigate the theoretical damping performance of a resonant shunt circuit, as well as the actual performance of an implemented PPF controller. These results will be presented in Section 3.4.

3.3.1. Experimental setup

In this section the experimental setup used for acquiring modal data to see the behaviour of the wafer gripper, as well as validating the implementation of active vibration control, will be provided. An overview of the setup is provided in Figure 3.4. The wafer gripper clamped with its aluminum clamp is suspended by an elastic cord from a steel frame. Essentially, the wafer gripper will be free-hanging. This configuration was chosen to analyze the behavior of the end-effector itself. The gripper is attached with a M5 bolt attached to a converter to a shaker (Brüel & Kjaer Vibration Exciter type 4809). This shaker excites the clamp of the gripper, and since the clamp has a considerable larger mass than

the thin wafer gripper, the wafer gripper can be considered to be clamped in this configuration. The dynamics of the gripper are of interest and therefore the chosen orientation of the gripper does not matter as gravity should not influence the results. A chirp signal is sent to the shaker, after which the displacement is measured at a pre-specified location on the wafer gripper. This measurement is done through the use of laser doppler scanning vibrometer (Polytec Scanning Vibrometer PSV-400). The vibrometer measures a high frequency signal which can be chosen to be decoded by different velocity or displacement decoders. The Polytec OFV-5000 Controller that comes with its own commercial software package, PSV-E-401 Junction Box, PSV-I-400 Scanning Head and PSV-W-401 PC are used to complete the scanning vibrometry setup.

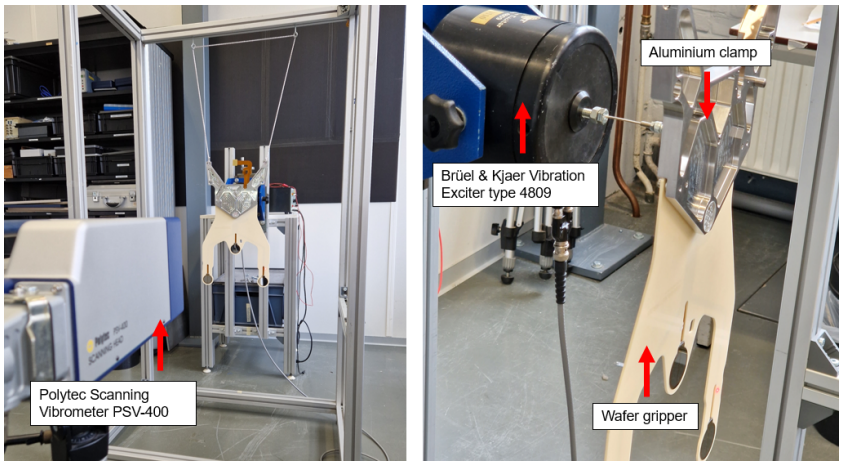

Figure 3.4: Experimental setup

3.3.2. Modal Analysis

Before implementing piezoelectric patches onto the gripper, the modal behaviour of the wafer gripper is analyzed. Firstly, a single point measurement is done by the laser Doppler vibrometer, where the tip velocity is measured when the wafer gripper is excited by the shaker. A chirp signal is sent to the shaker in order to perform system identification up to 100Hz, where the output of the vibrometer is taken over the reference signal coming from the shaker. To get a full signal from the vibrometer, reflective tape (ifm electronic E21015) is used to increase the reflectivity of the surface.

Figure 3.5: Wafer gripper with reflective tape for a single point measurement

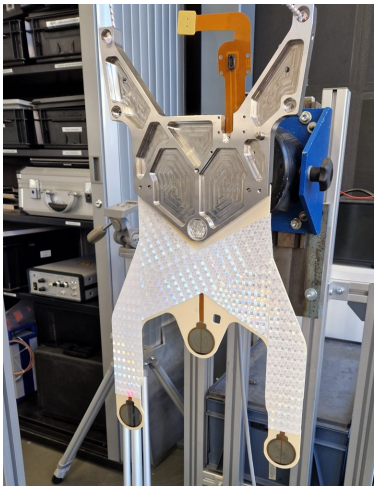

Figure 3.6: Wafer gripper completely covered with reflective tape

To check whether or not the mass of the tape added to the gripper changes the dynamics of the system, a small piece of tape is applied first, see Figure 3.5. After this, the entire surface is covered with

reflective tape as in Figure 3.6. To check the initial behavior of the wafer gripper, the transfer function for a single piece of tape is depicted in Figure 3.7. The transfer function is from the output of the laser measurement at the tip of the gripper to the input chirp signal sent to the shaker. From the plot there can be seen that the two modes with the largest magnitude occur at around 58Hz and 76Hz. Therefore, the decision was made to target these modes for dampening the system. From Table 3.1, there can be seen that the added reflective tape slightly shifts the eigenfrequencies and the magnitudes. However, the change is considered to be small and the decision was made to continue with using the reflective tape on the surface of the gripper.

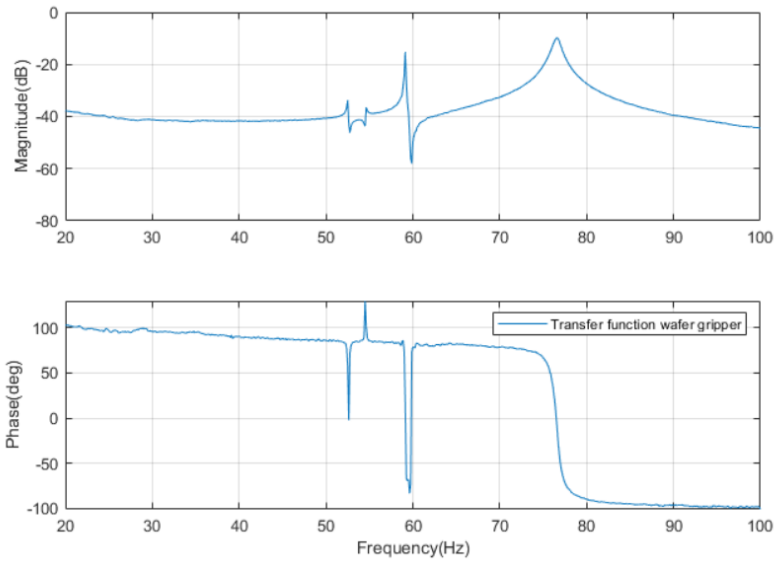

Figure 3.7: Bode plot of the wafer gripper with a small piece of reflective tape

Table 3.1: Modal analysis data for gripper covered with reflective tape

	Eigenfrequency (Hz)		Magnitude (dB)	
	1st mode	2nd mode	1st mode	2nd mode
small piece of tape	59.1	76.6	-15.1	-9.7
fully covered with tape	58.9	76.4	-20.4	-11.2

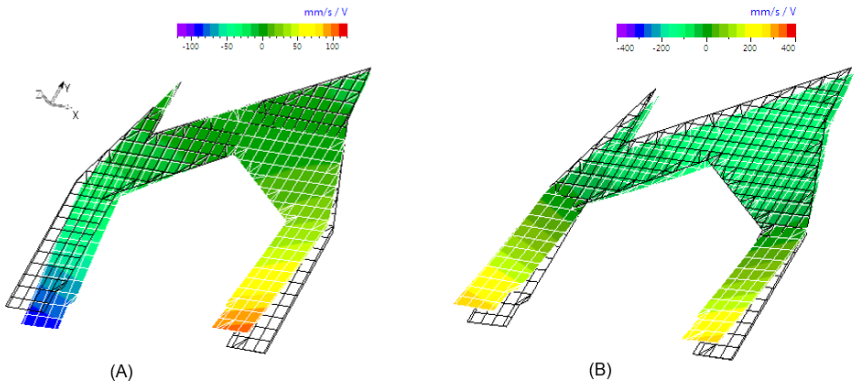

Figure 3.8: Modal analysis of wafer gripper at (A) 58.9Hz and (B) 76.4Hz

Each point on the surface is scanned using a grid. In this way, the mode shapes can be scanned

that are in turn plotted in Figure 3.8. These figures are then used to analyze the mode shapes and see how the gripper behaves at the eigenfrequencies of interest.

3.3.3. Optimal placement of piezoelectric transducers

Another important design choice for obtaining a damped system, is the placement of the piezoelectric actuators. After having chosen the type of piezoelectric actuators, the dimensions of the actuator are known. Looking at Equation 3.2, the only variable that is related to the placement of the piezoelectrics that remains unknown is $\Delta\theta_i^2$. This value indicates the difference in the slope of the mode shape at the beginning of the piezoelectric patch (θ_1) and the end of the patch (θ_2). Since the other parameters are constants, the coupling factor can be set proportional to the difference in the slopes of the mode shape, see Equation 3.7.

$$K_i \propto (\theta_1 - \theta_2) \tag{3.7}$$

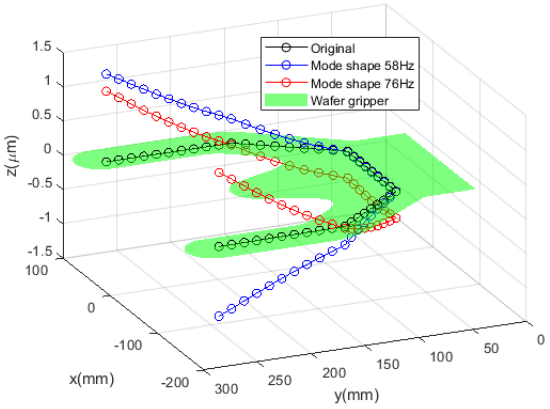

Figure 3.9: Mode shape displacement plot of wafer gripper

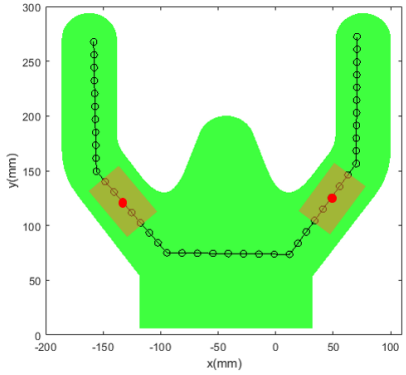

Figure 3.10: Geometry of wafer gripper with optimal piezopatch location

Using this relation, the placement of the piezoelectric patches can be determined, by finding the points on the wafer gripper where this value for K_i is the largest. For this, the mode shape data of the gripper for the targeted eigenmodes will be used. To get an initial idea for the placement, we limit location options. The displacement data for the mode shapes was taken along a line, as shown in Figure 3.9. This was done to simplify the optimization and reduce computational time, whilst still contributing to a 'proof of concept'. From the modal analysis data in Section 3.3.2, there can be seen that the eigenmodes mostly influence the behavior of the fingers of the wafer gripper,therefore the line was chosen such to cross the area with the most displacement, which in turn are the areas where the strains are expected to be largest. Computing the slopes of the mode shape at each location and looking for where K_i is maximal, the optimal placement along the specified line is provided in Figure 3.10.

3.3.4. Implementation of piezoelectric transducers

Now that the location of the piezoelectric transducers has been determined, they can be attached to the host structure. The gripper is covered in reflective tape, making sure to leave enough space for the piezoelectric patches and the wiring.

The glue used for attaching the piezoelectric patches is Loctite 401. This glue was chosen because of its high stiffness and ability to bond to different types of surfaces. The wires were then soldered with soldering paste to limit the heat applied to the electrodes as much as possible. This was mainly done to prevent the laminated polymer from deforming, which is important to have a nice flat surface to glue to the gripper. In Section 3.3.2, the influence of the reflective tape has been investigated. To check whether or not the piezoelectric patches influence the dynamics of the wafer gripper significantly, a single point measurement, same as to the measurement done in Section 3.3.2, was performed. In Figure 3.11 the wafer gripper is shown with and without piezoelectric patches and in Figure 3.12 the two transfer functions are shown. Looking at the frequencies of interest, there can be seen that the peak

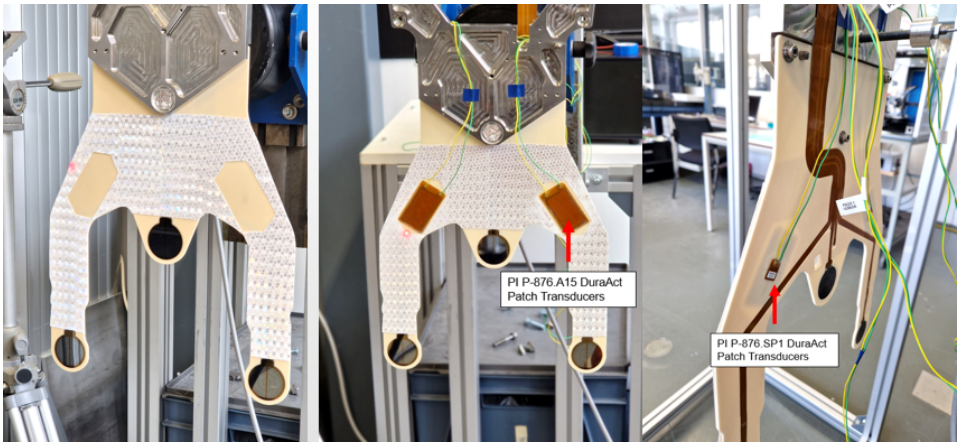

Figure 3.11: The wafer gripper with and without piezoelectric patches

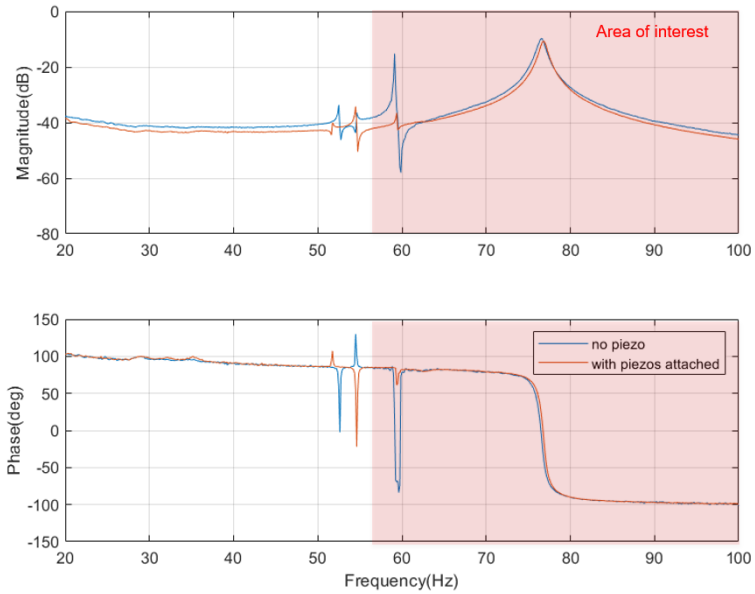

Figure 3.12: Bode plot of the wafer gripper with and without piezoelectric patches

at 58Hz has been significantly reduced, which could mean that the added stiffness of the piezoelectric patches has introduced damping of the eigenmode at 58Hz. The peak at around 76Hz has slightly shifted, but remains of roughly the same magnitude. Therefore, the focus will be to actively dampen the peak at around 76Hz with the use of a PPF controller.

In Figure 3.13 the full active setup is depicted. The piezoelectric actuators are each connected to a voltage amplifier that in turn are connected to a voltage source and a micro controller with a Simulink interface. On the backside of the gripper the piezoelectric sensors (P-876.SP1 DuraAct Patch Transducers) are attached at the same location as the actuators to ensure collocation. The first step to design an appropriate PPF controller is to identify the system using the piezoelectric pairs. System identification is performed by sending a chirp signal to one actuating piezo patch and then sensing the output using the two piezoelectric sensors on the backside of the gripper. Thus, in total 4 transfer functions can be acquired. These transfer functions are provided in Figure 3.14, together with the tuned PPF controller and the closed loop transfer functions. The PPF controller was designed for an eigenfrequency of 76.7Hz, as this is the frequency at which the second mode of interest occurs, when performing system identification with the piezoelectric patches.

The first row of plots show the collocated and non-collocated transfer functions, where the behavior is symmetric and as expected. High-pass behavior from the piezoelectric patches can be seen, after

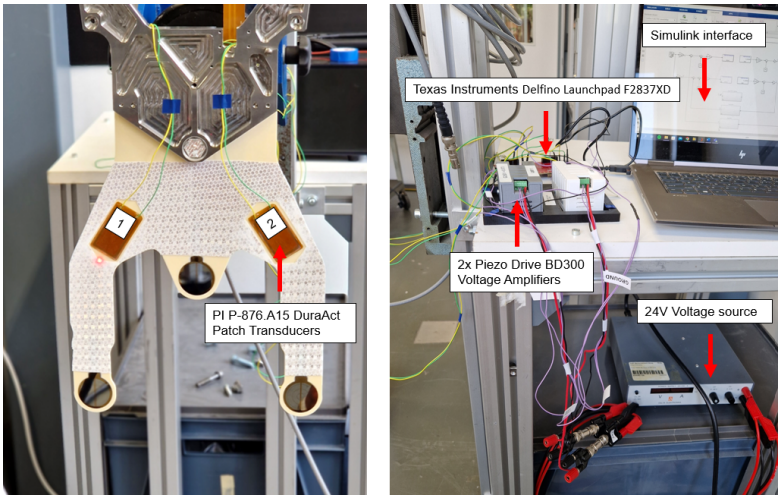

Figure 3.13: Experimental setup for active vibration control

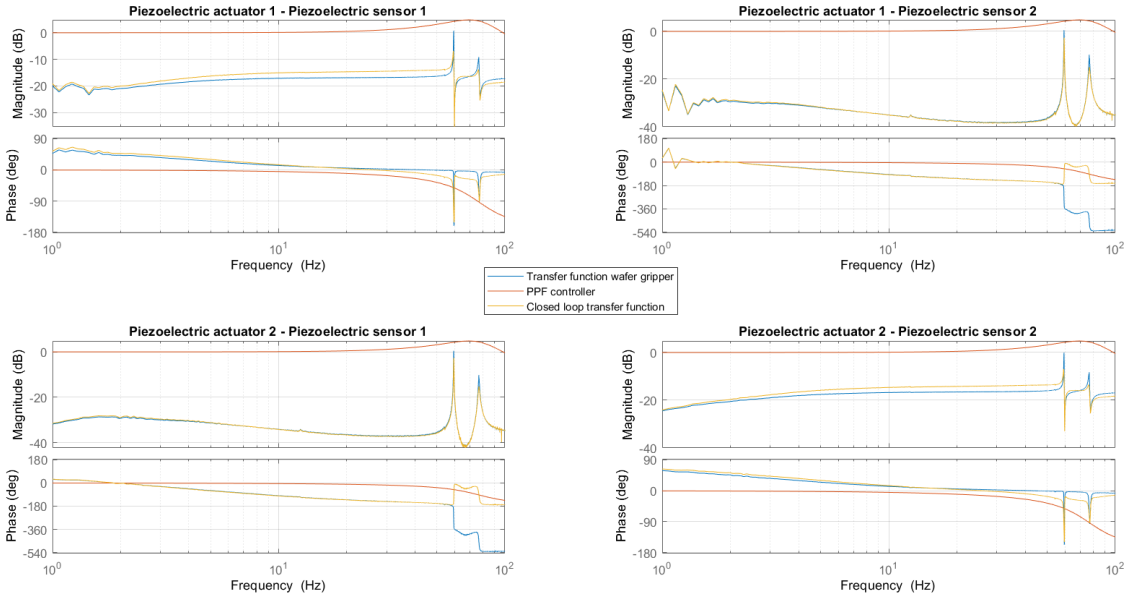

Figure 3.14: Transfer functions for the different piezoelectric pairs together with the designed PPF controller

which the eigenmodes of interest are shown. From the non-collocated transfer functions, non-minimal phase behavior can be seen as well, which is typical for these kinds of systems [4]. It should be noted that the plots in Figure 3.14 have a larger magnitude for the peak around 58Hz than in Figure 3.12. This means that the eigenmode at 58Hz can not be measurement by the non-collocated measurement with the Polytec scanner at the tip of the wafer gripper, see Figure 3.12. However, the mode can be observed when using the piezoelectric patches. This does not pose as a problem, because it is important that mainly the tips of the gripper are dampened since that is where the wafer will be attached to when moving it from A to B in the lithography machine.

3.4. Results

In this section the results will be presented from the Polytec Scanning Doppler Vibrometer PSV-400. To give an indication of how promising shunting is as a damping method, the coupling factor has been experimentally measured to provide theoretical values on the achievable damping.Furthermore, the results for the implemented PPF controller are provided.

3.4.1. Piezoelectric shunting

From Equation 3.5 in Section 2.3, the maximal theoretical damping value for a resistive and resonant shunt can be determined, respectively. To compute the coupling factor, the eigenfrequency for open-circuited electrodes (Ω) and short-circuited electrodes (ω) are measured by performing a single-point measurement for each configuration. The results for the experimentally measured coupling factor and maximal achievable theoretical damping for both a resistive and resonant shunt are provided in Table 3.2.

Table 3.2: Maximal achievable damping for a resistive and resonant shunt circuit tuned at 76Hz

	$\Omega(rad/s)$	$\omega(rad/s)$	K_i^2
Measured parameters	76.8	76.7	0.0026

	$\zeta_{max}(\%)$
Resistive shunt	0.065
Resonant shunt	2.6

3.4.2. Active vibration control

The PPF controller was implemented by setting the eigenfrequency at 76.7Hz. The damping ratio was set at 0.3, which is a typical value used for PPF controllers [4]. The gain was slowly increased to see the effect of the PPF controller on the damping performance of the system. In Table 3.3 the damping performance for different gains is provided.

Table 3.3: Damping values for different PPF gains

Gain	Q-factor	Damping (%)
0.1	22.9	2.2
0.2	17.6	2.8
0.3	15.7	3.2
0.4	15.2	3.3
0.5	15.2	3.3

In Figure 3.15 the measured transfer functions of the wafer gripper are provided. From the Figure there can be seen that the magnitude of the peak decreases with an increased gain. The gain could not be further increased past 0.5, since the for higher values the system became unstable.

System identification has been performed with one of the piezoelectric actuator-sensor pairs to check the behavior for higher gains. In Figure 3.16 the bode plots are provided for a gain of 0.2 and a gain of 0.5. It can be seen that for a higher gain the stiffness line exceeds the magnitude of the eigenmodes at 58Hz and 76Hz, which is not the case for a gain of 0.2.

3.5. Discussion

From the Results in Section 3.4 there can be seen that the eigenmode at 76.7Hz is being dampened through the use of active control. The damping behavior is as expected, as the plot shows a reduction in the magnitude of the peak. There is a slight shift of the resonance peak to the left, which could be due to the added gain that introduces an additional stiffness to the system.

The gain has not been further increased beyond a gain of 0.5, because the system became unstable when doing so, which prevented the measurement from being performed. This could have several possible reasons. It could be that something in the experimental setup causes this behavior, for example noise in the voltage amplifiers that cause instability. However, it could also be that there are some unknown dynamics in the system. In an attempt to find a reason for why this happens we look at Figure 3.16 where we see that the gain at 0.5 is already too high of a gain. Namely, the resonance peaks are almost completely dampened and significantly below the stiffness line of the plot. This means that it seems like the piezoelectric transducers cannot dampen the resonance peaks any further, whilst the mode is still visible when measuring the system with the laser Doppler vibrometer. It is interesting to

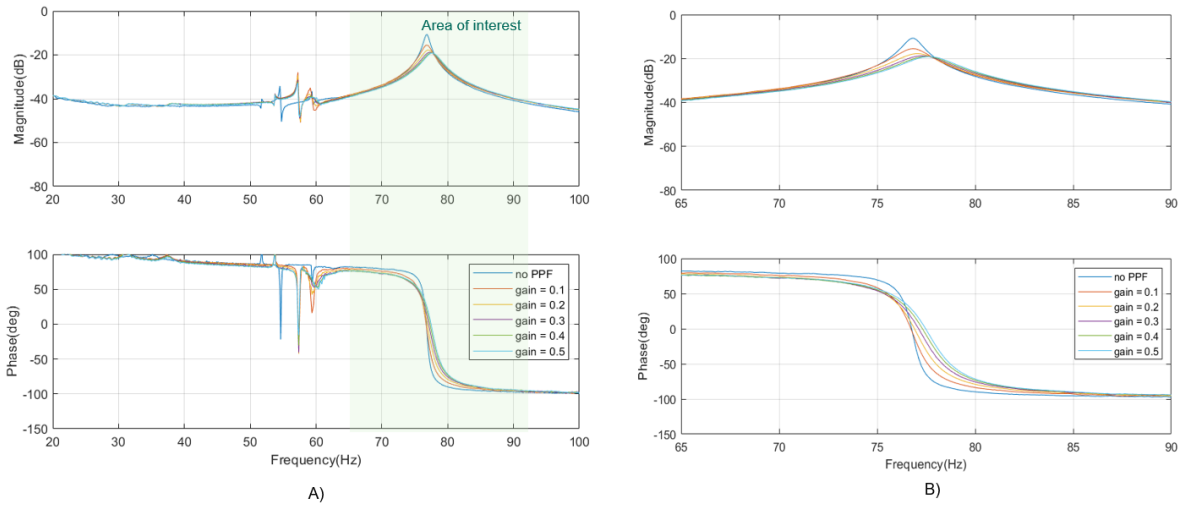

Figure 3.15: Bode plots for a system with a implemented PPF controller: A) Entire plot B) Zoomed-in plot showing the eigenmode around 76Hz

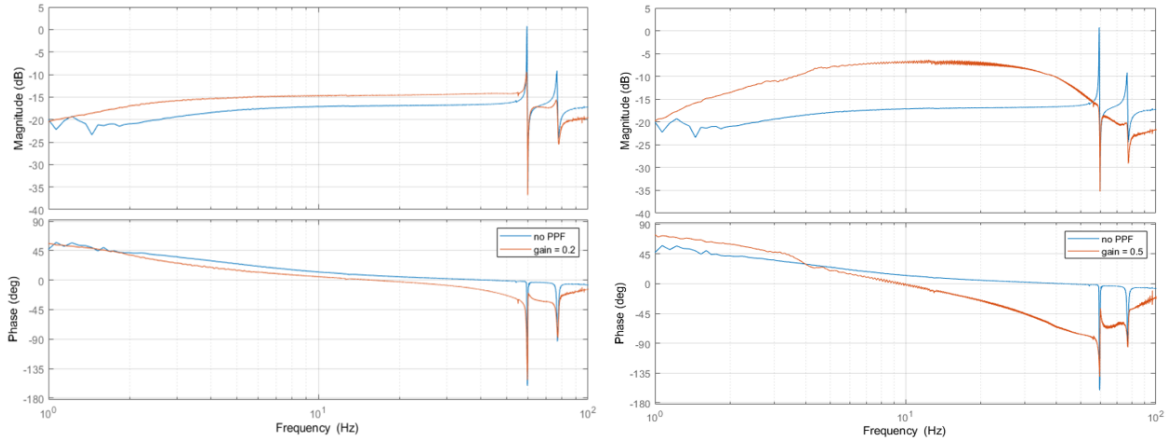

Figure 3.16: Transfer function of piezoelectric sensor 1 to piezoelectric actuator 1 for a gain of 0.2 and 0.5 (left to right)

see this difference in observability for the collocated piezoelectric pairs and the non-collocated measurement done with the Polytec scanning vibrometer. It could be argued that the configurations and placement of the piezoelectric patches should be altered to effectively perform damping at the tip of the wafer gripper.

It should be noted that the piezoelectric actuators have not saturated for a gain of 0.5, since the actuators can go up to 300V with the current setup which is not reached for a gain of 0.5. Additionally, the stability conditions from Equation 3.6 is still satisfied. Therefore, it remains unknown where this unstable behavior is coming from. Nevertheless, the current results in Table 3.3 seem to be promising. With a simple second order low-pass filter the peak at 76Hz is already dampened for 3.3%. There could be argued that improvement of the controller could significantly increase the percentage of modal damping even more. This improvement could be done by tuning the damping and frequency parameters more accurately or by making the controller more adaptive, for example. Another interesting topic would be to see if another or a combination of control algorithms would increase the percentage of modal damping.

Additionally, the placement of the piezoelectric patches has been performed along a line, whilst endless data points could be measured using the Polytec laser vibrometer. The possibility exists that if we optimize the placement along the surface of the gripper, there might be another better solution to the optimal placement of the piezoelectric patches. As mentioned in Section 3.3.4 the added stiffness of piezoelectric patches dampened the first mode of interest at 58Hz, solely because of their placement.

The reason why this happens and how the placement is related to this added damping should be further investigated. It could be interesting to know how the relation is, in order to design an effectively dampened system.

Lastly, it can be noted that the scope of the research is set at the modes of interest that were determined in Section 3.3.2. But there is some change in behavior happening for the lower frequency modes (modes below 58Hz) when looking at Figure 3.15. These modes were left out of scope as the focus was set on the two largest modes and the smaller modes do not seem to have a larger magnitude than the modes of interest at 58Hz and 76Hz. Additionally, since these modes are so small they are harder to measure as well. For future work the behavior that is seen for the lower frequency modes could be further investigated.

3.6. Conclusion

In this chapter, a design has been proposed to effectively dampen two eigenmodes of a state-of-the-art wafer gripper end-effector. Several experiments have been performed to check the modal behavior of the wafer gripper. Using this data a design has been proposed to perform active vibration control. The goal to design a system to achieve at least 5% of modal damping for two eigenmodes has not been satisfied, as for the second mode of interest at 76Hz, the maximum modal damping achieved was 3.3%. However, 3.3% damping was achieved with a simple PPF controller with a limited gain for which the piezoelectric transducers where placed according to a simplified line optimization. This shows that the concept of dampening very stiff and thin end-effectors, such as the wafer gripper, is promising.

4

Conclusion and Future work

This project shows one of the few industrial design applications of piezoelectric transducers to a thin end-effector with a high stiffness. A novel design has been proposed to dampen two eigenmodes of a state-of-the-art wafer gripper, one of which was successfully dampened using positive position feedback. This was motivated by the increasing demands on the performance of the wafer gripper, where the goal was set to achieve at least 5% modal damping for its eigenmodes. This objective served as a 'proof of concept' to show the possibilities of implementing a state-of-the-art damping method to an industrial application, incentivizing the use of piezoelectric materials for other similar structures. A literature study was performed to scan the field and investigate different possible solutions to dampen the wafer gripper. A systematic overview of current trends in terms of dampening thin structures was provided, where the use of smart materials and structures were emphasized. It became evident that nowadays piezoelectrics are best suited for the integration on thin structures, due to their dimensions and maturity in the market, meaning that the transducers are easily commercially available. In order to design a dampened system, the basic principles on the electromechanical behaviour of piezoelectric materials were studied, where a back-of-the-envelope formula for the electromechanical coupling factor has been provided that can be optimized for a smart structure including piezoelectric materials. Shunting and active vibration control are proposed damping methods that could be implemented to provide modal damping to a thin structure. However, for shunting the limitation is that the circuits tend to use high inductance values for low frequencies, which poses as a practical limitation. Therefore, the choice was made to perform active vibration control using a PPF control algorithm to the wafer gripper. First, the dynamics of the wafer gripper were studied, after which this data was used together with the electromechanical coupling relation to determine the dimensions and placement of the piezoelectric transducers. An experimental setup has been built to check the modal behaviour for the gripper to design an appropriate system. The same setup was then used to check the performance of the active setup. The designed damping method showed a maximal achievable modal damping performance of 3.3% The goal to design a system to achieve at least 5% of modal damping for two eigenmodes has not been satisfied. However, it should be noted that 3.3% damping was achieved with a simple PPF controller with a limited gain for which the piezoelectric transducers where placed according to a simplified line optimization. This shows that the concept of dampening very stiff and thin end-effectors is promising and that eigenmodes can be successfully dampened using active vibration control.

4.1. Future steps

In this work there are several aspects that could be improved which all relate to the design of the dampened system and its experimental setup. The first aspect is related to the design of the placement of the piezoelectric transducers. The placement was determined by using the relation of the mode shapes and the electromechanical coupling factor. The coupling factor was then optimized along a line to determine the optimal placement. However, with the Polytec laser Doppler vibrometer all points of the gripper can be scanned to obtain its modal data. Therefore, the optimization of the piezoelectric transducers could also be performed along the entire surface of the gripper. In this way the optimal orientation and geometry of the piezoelectric transducers can be optimized to obtain a better mechanical

design. Another aspect of the mechanical design that could be studied, is the material and design of the wafer gripper itself. The gripper has been made to be very stiff to shift the eigenfrequencies beyond their excitation band, but by adding the piezoelectric patches there could be argued if the high stiffness is still required. Also, there could be looked into integrating the piezoelectric transducers into the host structure, instead of attaching them on the gripper. Namely, attaching them on the gripper increases the thickness.

Additionally, improvements could be made on the controller. More time could be spent on tuning the current PPF controller to achieve a higher damping. Furthermore, there could be looked into more advanced controllers which could possibility increase the maximal achievable modal damping performance. Different algorithms, such as direct velocity feedback or integral force feedback could be investigated as well. There could also be looked into non-collocated control to dampen the system more effectively. The current experimental setup serves as a good basis to test these different control algorithms.

Lastly, it is interesting to further investigate the modal behavior of the gripper for different eigenfrequencies as well. This to really understand the dynamics of the wafer gripper in order to achieve a better overall design.

Bibliography

1. Javier Yanes. *The Future of Electronics: Is it Time to Declare the End of Moore's Law?* May 2020. https://www.bbvaopenmind.com/en/science/physics/the-future-of-electronics-is-it-time-to-declare-the-end-of-moores-law/.
2. Gripp, J. A. & Rade, D. A. *Vibration and noise control using shunted piezoelectric transducers: A review* Nov. 2018.
3. Li, S., Ochs, S., Slomski, E. & Melz, T. *Design of control concepts for a smart beam structure with sensitivity analysis of the system* in *Computational Methods in Applied Sciences* **43** (Springer Netherland, 2017), 115–132. ISBN: 9783319445052.
4. Preumont, A. *Vibration Control of Active Structures: An Introduction* 4th. ISBN: 978-3-319-72295-5 (Springer, 2018).
5. Baz, A. M. in *Active and Passive Vibration Damping* 1st. Chap. 1 (John Wiley & Sons, 2019).
6. Wang, Z., Gao, H., Wang, H. & Chen, Z. Development of stiffness-adjustable tuned mass dampers for frequency retuning. *Advances in Structural Engineering* **22,** 473–485. ISSN: 20484011 (Jan. 2019).
7. Zheng, W., Lei, Y., Li, S. & Huang, Q. Topology optimization of passive constrained layer damping with partial coverage on plate. *Shock and Vibration* **20,** 199–211. ISSN: 10709622 (2013).
8. Syriac, R. M., Bhasi, A. B. & Rao, Y. V. *A review on characteristics and recent advances in piezoelectric thermoset composites* 2020.
9. Qiu, Z. c., Han, J. d., Zhang, X. m., Wang, Y. c. & Wu, Z. w. Active vibration control of a flexible beam using a non-collocated acceleration sensor and piezoelectric patch actuator. *Journal of Sound and Vibration* **326,** 438–455. ISSN: 0022460X (Oct. 2009).
10. Heganna, S. S. & Joglekar, J. J. *Active Vibration Control of Smart Structure Using PZT Patches* in *Procedia Computer Science* **89** (Elsevier B.V., 2016), 710–715.
11. Tuma, J., Strambersky, R. & Pavelka, V. *Modeling the Use of the Patch Piezo-Actuators for Active Vibration Control* in (Institute of Electrical and Electronics Engineers (IEEE), June 2021), 1–4. ISBN: 9781728186092.
12. Shivashankar, P. & Gopalakrishnan, S. *Review on the use of piezoelectric materials for active vibration, noise, and flow control* May 2020.
13. Zheng, Q., Richter, H. & Gao, Z. Active disturbance rejection control for piezoelectric BEAM. *Asian Journal of Control* **16,** 1612–1622. ISSN: 19346093 (Nov. 2014).
14. Cho, C. & Pan, Q. *Damping Property of Shape Memory Alloys Mechanical properties of CFRP View project High performance automotive brake disk development View project DAMPING PROPERTY OF SHAPE MEMORY ALLOYS* tech. rep. (2008). https://www.researchgate.net/publication/281792397.
15. Janocha, H. in *Adaptronics and Smart structures* 95–300 (Springer, 2007).
16. Lagoudas, D. C. *Shape Memory Alloys* ISBN: 978-0-387-47684-1. http://link.springer.com/10.1007/978-0-387-47685-8 (Springer US, Boston, MA, 2008).
17. Damanpack, A. R., Bodaghi, M., Aghdam, M. M. & Shakeri, M. On the vibration control capability of shape memory alloy composite beams. *Composite Structures* **110,** 325–334. ISSN: 02638223 (Apr. 2014).
18. Sun, Y., Fang, D. & Soh, A. K. Thermoelastic damping in micro-beam resonators. *International Journal of Solids and Structures* **43,** 3213–3229. ISSN: 00207683 (May 2006).
19. Graf, C. & Maas, J. *Electroactive polymer devices for active vibration damping* in *Electroactive Polymer Actuators and Devices (EAPAD) 2011* **7976** (SPIE, Mar. 2011), 79762I. ISBN: 9780819485380.

20. Wolf, K., Röglin, T., Haase, F., Finnberg, T. & Steinhoff, B. *An electroactive polymer based concept for vibration reduction via adaptive supports* in *Electroactive Polymer Actuators and Devices (EAPAD) 2008* **6927** (SPIE, Mar. 2008), 69271F. ISBN: 9780819471130.
21. Silva, E. P. Beam shape feedback control by means of a shape memory actuator. *Materials and Design* **28,** 1592–1596. ISSN: 18734197 (2007).
22. Moheimani, R. S. & Fleming, A. J. *Piezoelectric Transducers for Vibration Control and Damping* (Springer, 2006).
23. Wang, H. & Jasim, A. in *Eco-efficient Pavement Construction Materials* 367–382 (Elsevier Inc., Jan. 2020). ISBN: 9780128189818.
24. Institute of Electrical and Electronics Engineers Inc. IEEE standard on piezo-electricity. ANSI/IEEE Std. 176–1987 (1988).
25. Bhalla, S. & Moharana, S. A refined shear lag model for adhesively bonded piezo-impedance transducers. *Journal of Intelligent Material Systems and Structures* **24,** 33–48. ISSN: 1045389X (Jan. 2013).
26. Robbins, M. F. in *Ultimate Electronics: Practical Circuit Design and Analysis* chap. 2.17 (CircuitLab, Inc., 2021).
27. Abdus, M., Quazi, S. & Rahman, M. *Fundamentals of Electrical Circuit Analysis* (Springer, 2018).
28. Han, L., Wang, X. D. & Sun, Y. The effect of bonding layer properties on the dynamic behaviour of surface-bonded piezoelectric sensors. *International Journal of Solids and Structures* **45,** 5599–5612. ISSN: 00207683 (Oct. 2008).
29. Tinoco, H. A., Serpa, A. L. & Ramos, A. M. Numerical Study of the Effects of Bonding Layer Properties on Electrical Signatures of Piezoelectric Sensors (2010).
30. Pietrzakowski, M. Active damping of beams by piezoelectric system: e□ects of bonding layer properties. *International Journal of Solids and Structures* **38,** 7885–7897. `www.elsevier.com/locate/ijsolstr` (2001).
31. Rosi, G., Paccapeli, R., Ollivier, F. & Pouget, J. Optimization of piezoelectric patches positioning for passive sound radiation control of plates. *Journal of Vibration and Control* **19** (2012).
32. Yan, B., Wang, K., Hu, Z., Wu, C. & Zhang, X. *Shunt Damping Vibration Control Technology: A Review* 2017.
33. Hagood, N. W. & Flotow, A. V. Damping of structural vibrations with piezoelectric materials and passive electrical networks. *Journal ofSound and Vibration* **146,** 243–268 (1991).
34. Andreaus, U. & Porfiri, M. Effect of electrical uncertainties on resonant piezoelectric shunting. *Journal of Intelligent Material Systems and Structures* **18,** 477–485. ISSN: 1045389X (May 2007).
35. Wu, S.-y. *Piezoelectric shunts with a parallel R-L circuit for structural damping and vibration control* in *Smart Structures and Materials 1996: Passive Damping and Isolation* **2720** (SPIE, May 1996), 259–269. ISBN: 0819420956.
36. Hollkamp, J. J. Multimodal Passive Vibration Suppression with Piezoelectric Materials and Resonant Shunts. *Journal of Intelligent Material Systems and Structures* **5** (1994).
37. Wu, S.-Y. Method for Multiple Mode Piezoelectric Shunting with Single PZT Transducer for Vibration Control. *Journal of Intelligent Material Systems and Structures* **9** (1998).
38. Behrens, S., Moheimani, S. O. & Fleming, A. J. Multiple mode current flowing passive piezoelectric shunt controller. *Journal of Sound and Vibration* **266,** 929–942. ISSN: 0022460X (Oct. 2003).
39. Sun, H. *et al.* Vibration suppression of a hard disk driver actuator arm using piezoelectric shunt damping with a topology-optimized PZT transducer. *Smart Materials and Structures* **18.** ISSN: 09641726 (2009).
40. Antoniou, A. & Naidu, K. S. Modeling of a Gyrator Circuit. *IEEE Transactions on Circuit Theory* **20,** 533–540. ISSN: 00189324 (1973).
41. Riordan, R. Simulated inductors using differential amplifiers. *Electron* **3,** 291 (1967).

42. Richard, C., Guyomar, D., Audigier, D. & Bassaler, H. *Enhanced semi-passive damping using continuous switching of a piezoelectric device on an inductor* in *Smart Structures and Materials 2000: Damping and Isolation* **3989** (SPIE, Apr. 2000), 288–299.

43. Clark, W. W. Vibration control with state-switched piezoelectric materials. *Journal of Intelligent Material Systems and Structures* **11,** 263–271. ISSN: 1045389X (Apr. 2000).

44. Fleming, A. J. & Moheimani, S. O. R. *Adaptive piezoelectric shunt damping* tech. rep. (2003).

45. Niederberger, D., Morari, M. & Pietrzko, S. *Adaptive resonant shunted piezoelectric devices for vibration suppression* tech. rep. (2003). `http://spiedl.org/terms`.

46. Gripp, J. A., Góes, L. C., Heuss, O. & Scinocca, F. An adaptive piezoelectric vibration absorber enhanced by a negative capacitance applied to a shell structure. *Smart Materials and Structures* **24.** ISSN: 1361665X (Nov. 2015).

47. Wang, X., Pereira, E., Díaz, I. M. & García-Palacios, J. H. Velocity feedback for controlling vertical vibrations of pedestrian-bridge crossing. Practical guidelines. *Smart Structures and Systems* **22,** 95–103. ISSN: 17381991 (July 2018).

48. Teo, Y. R. & Fleming, A. J. Optimal integral force feedback for active vibration control. *Journal of Sound and Vibration* **356,** 20–33. ISSN: 10958568 (Nov. 2015).

49. Friswell, M. I. & Inman, D. J. Relationship between positive position feedback and output feedback controllers. *Smart Materials and Structures* **8,** 285–291. ISSN: 09641726 (June 1999).

50. Chopra, I. *Review of state of art of smart structures and integrated systems* 2002.

51. Behrens, S., Fleming, A. J. & Moheimani, S. O. R. *A broadband controller for shunt piezoelectric damping of structural vibration* tech. rep. (2003).